AGU PUBLICATIONS

JGR

Journal of Geophysical Research: Space Physics

RESEARCH ARTICLE
10.1002/2016JA023444

Key Points:
- Solar activity variation of the plasmaspheric density is rather small compared with the ionosphere
- Fairly significant longitudinal variation exists in the equatorial plasmasphere
- Plasmaspheric TEC distributions do not linearly follow the ionosphere despite strong coupling processes between the two regions

Correspondence to:
G. Jee,
ghjee@kopri.re.kr

Citation:
Shim, J. S., G. Jee, and L. Scherliess (2017), Climatology of plasmaspheric total electron content obtained from Jason 1 satellite, *J. Geophys. Res. Space Physics*, *122*, doi:10.1002/2016JA023444.

Received 9 SEP 2016
Accepted 7 JAN 2017
Accepted article online 25 JAN 2017

Climatology of plasmaspheric total electron content obtained from Jason 1 satellite

Ja Soon Shim[1], Geonhwa Jee[2], and Ludger Scherliess[3]

[1]CUA/NASA GSFC, Greenbelt, Maryland, USA, [2]Korea Polar Research Institute, Incheon, South Korea, [3]Center for Atmospheric and Space Sciences, Utah State University, Logan, Utah, USA

Abstract We used more than 40 million total electron content (TEC) measurements obtained from the GPS TurboRogue Space Receiver receiver on board the Jason 1 satellite in order to investigate the global morphology of the plasmaspheric TEC (pTEC) including the variations with local time, latitude, longitude, season, solar cycle, and geomagnetic activity. The pTEC corresponds to the total electron content between Jason 1 (1336 km) and GPS (20,200 km) satellite altitudes. The pTEC data were collected during the 7 year period from January 2002 to December 2008. It was found that pTEC increases by about 10–30% from low to high solar flux conditions with the largest variations occurring at low latitudes for equinox. During low solar flux condition, pTEC is largely independent of geomagnetic activity. However, it slightly decreases with increasing geomagnetic activity at low latitudes during high solar flux. The seasonal variations such as the annual and semiannual anomalies in the ionosphere also exist in the low-latitude plasmasphere. In particular, the American sector (around 300°E) shows strong annual asymmetry in the plasmaspheric density, being larger in December than in June solstice.

1. Introduction

The plasmasphere is a region of relatively dense and cold plasma ($n \sim 10^8$ m^{-3}, $E \sim 1$ eV) in the inner part of the magnetosphere while it can also be considered to be a continuation of the ionosphere into the magnetosphere. The boundary between both regions is defined as the transition from O^+ to H^+ as the primary ion constituent and it occurs at the altitude region of about 500 to 2000 km, depending on geophysical conditions. Since the density distributions of the plasmasphere is determined by very different physical mechanisms from the ionosphere, the existence of the plasmasphere makes it difficult to interpret the data from the ionospheric measurements such as GPS total electron content (TEC) [*Yizengaw et al*., 2008; *Mazzella*, 2009; *Bishop et al*., 2009; *Thompson et al*., 2009; *Jee et al*., 2010]. The GPS TEC includes not only the ionosphere but also the most part of the plasmasphere, and it is essential to know the plasmaspheric contribution to GPS TEC for its applications for the ionospheric studies. Furthermore, the coupling between both regions is known to greatly influence not only the plasmaspheric density but also the ionospheric density [*Carpenter and Park*, 1973; *Horwitz et al*., 1986; *Singh and Singh*, 1997; *Sandel and Denton*, 2007]. There are a number of studies on the plasmaspheric density distributions from observations and numerical modelings [*Park*, 1973; *Park*, 1974; *Park et al*., 1978; *Clilverd et al*., 1991; *Guiter et al*., 1995; *Ganguli et al*., 2000; *Richards et al*., 2000; *Belehaki et al*., 2004; *Webb and Essex*, 2004; *Clilverd et al*., 2007; *Yizengaw et al*., 2008; *Lee et al*., 2013; *Huba and Krall*, 2013]. However, the observation for the plasmaspheric density is very limited, and therefore, the plasmaspheric TEC data obtained from Jason 1 satellite provide a valuable opportunity to investigate the characteristics of the plasmaspheric density distribution.

Jason 1 is the successor to the TOPEX/POSEIDON mission that had been observed ocean surface topography from 1992 through 2005. Like its predecessor, Jason 1 mission is a joint project between the National Aeronautics and Space Administration (NASA, United States) and the Centre National d'Etudes Spatiales (France) space agencies [*Fu et al*., 1994]. Jason 1 orbits the Earth at an altitude of 1336 km with an inclination angle of 66° and a period of 112 min. There are 127 orbits in each 9.916 day period, which means that the satellite passes vertically over the same location, to within 1 km, about every 10 days. The satellite orbits are close to Sun-synchronous and advance by 2° per day. Consequently, it takes about 90 days to cover all local times. Jason 1 uses a dual-frequency radar altimeter operating simultaneously at 13.6 GHz (Ku band) and 5.3 GHz (C band) to observe the surface height of the oceans. The TEC measurements obtained from the down-looking dual-frequency radar altimeter are essentially equivalent to the TEC of the ionosphere in a vertical column extending from the subsatellite reflection point on the surface of the ocean to the height

of the satellite at 1336 km altitude, and the TEC observations have been used to study the general morphology and variability of the ionosphere [*Codrescu et al*., 1999, 2001; *Jee et al*., 2004; *Vladimer et al*., 1999; *Scherliess et al*., 2008]

Jason 1 also has a GPS receiver, TRSR (TurboRogue Space Receiver). The TRSR is a high-performance GPS receiver designed to provide backup precise orbit determination for Jason 1. It measures precise GPS pseudorange and continuous carrier phase data from up to 12 GPS satellites (about six satellites on the average). The total electron content (TEC) obtained from the pseudorange and carrier phase data provided by TRSR corresponds to the slant TEC of the plasmasphere at altitudes from 1336 km to 20,200 km. In this study, for the first time, the plasmaspheric TEC (pTEC) measurements through an up-looking antenna onboard Jason 1 satellite are used to investigate the plasmaspheric TEC climatology. The pTEC measurements are briefly described in the next section, and the results of the analysis are presented in section 3. Finally, summaries as well as conclusions are presented in section 4.

2. GPS TEC Measurement From Jason 1

In order to investigate the general plasmaspheric TEC morphology, we used the Jason 1 GPS pTEC measurements that were provided by Archiving, Validation, and Interpretation of Satellite Oceanographic data. The Jason 1 pTEC data are taken every 30 s and available from 15 January 2002 to 31 December 2008. The TRSR GPS receiver on board the Jason 1 takes each data from six GPS satellites on average (up to 12 GPS satellites). Thus, our data set consists of more than 40 million pTEC values (7 years × 365 days × 24 h/d × 60 min/h × 2 times/min × 6 GPS satellites).

Plasmaspheric slant TEC values were obtained from pseudorange and carrier phase data from multiple GPS satellites. The slant TEC data from different viewing geometries were combined by mapping to the vertical direction using the so-called thin-shell approximation, which is similar to the ionospheric shell approximation [*Mannucci et al*., 1993]. The median height of the plasmasphere (shell height) was determined by the physics-based ionosphere-plasmasphere model, which is about 2000 km above the altitude of Jason 1 satellite. For the calculation of the plasmaspheric shell height, we assume that the plasmasphere starts from this satellite altitude. In order to reduce the error associated with the mapping procedure and multipath, the selected TEC data were restricted to the elevation angles above 60°. One of the largest sources of error in the analysis of the TEC data is satellite biases, and this bias was subtracted from the slant TEC values before the slant TEC was converted to vertical TEC. However, since it was not available, the bias of the receiver TRSR was obtained by assuming that the minimum vertical TEC value is zero, which possibly occurs in the high-latitude regions. We found that the minimum values occur in the geomagnetic latitude range from ±50° to ±70°. It should also be noted that the Jason 1 GPS pTEC may not necessarily be the optimum observation to represent the plasmaspheric total electron content due to the fact that the transition height of O^+-H^+ can significantly be varied with geophysical conditions approximately within 500 to 1500 km altitude although the transition height mostly stays below the Jason 1 satellite orbit [*Kutiev et al*., 1994; *Marinov et al*., 2004; *Kutiev and Marinov*, 2007].

Figure 1a shows a scatterplot of daily minimum vertical pTEC and the median values (denoted by black squares) as well as the upper and lower quartile values as a function of day of year (DOY) during the period from 2002 to 2008. The median and average values of daily minimum vertical pTEC were obtained every 30 days with a 90 day wide bin. The average values are hardly different from the median values and are not shown here. An error in the plateau region of the curve (about from 2004/150 to 2006/180) is about 0.2 total electron content unit (TECU; 1 TECU = 10^{16} el/m^2). An error is relatively large (up to about 0.5 TECU) in the regions with large gradients. For example, a relatively large error and increased scatter are seen around the end of 2006. It could possibly be related to a switch of receivers from TRSR1 to TRSR2 due to TRSR1 failure in September 2006.

Our study period (2002–2008) includes the maximum and declining phase of solar cycle 23. In order to investigate whether the decrease of daily minimum pTEC over time is related to the decrease of solar flux or not, we plotted the daily minimum pTEC (black dots) and $F_{10.7\ cm}$ solar flux values (crosses) as a function of day of year for 2003 in Figure 1b. It is found that the daily minimum pTEC seems not to be correlated with solar activity condition. Therefore, the daily minimum pTEC can be used as a receiver bias without contamination of pTEC variations with solar activity condition. The average values of daily minimum pTEC over 90 days were

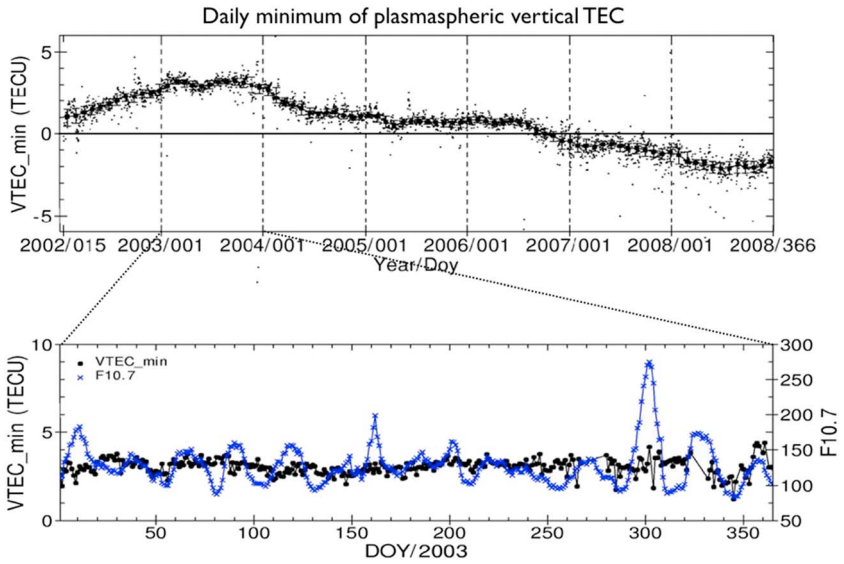

Figure 1. (a) Scatterplot for daily minimum values of the plasmaspheric TEC as a function of DOY during the period from 2002 to 2008. The median values of daily minimum TEC (black squares), as well as the upper and lower quartile values, are shown. (b) Daily minimum values of the plasmaspheric TEC (black circles) and $F_{10.7}$ solar flux values (crosses) for the year of 2003.

used as a receiver bias for the 30 days in the middle of 90 day period. Although there is a possibility to underestimate or overestimate the plasmaspheric TEC values by using the calculated biases, however, the general morphology of the resulting plasmaspheric TEC would not be affected.

For the study of the general TEC morphology of the plasmasphere, the data were binned as shown in Table 1. We used the same binning criteria as used in the previous ionospheric TEC morphology study done by *Jee et al*. [2004] to compare with the results of this study. The data are sorted into magnetic local time (MLT), magnetic latitude, geomagnetic activity, solar activity, and seasonal bins. We choose a bin size of 2° × 15 min resolution in magnetic latitude and magnetic local time. *Kp* and $F_{10.7}$ indices are chosen for the geomagnetic and solar activities, respectively. The data are sorted into three levels of geomagnetic activity: low ($Kp \leq 1.7$, Kp_ave = 1.0), medium ($2.0 \leq Kp \leq 3.3$, Kp_ave = 2.5), and high ($Kp \geq 3.3$, Kp_ave = 3.9) geomagnetic activities. $F_{10.7}$ bins have two levels: low ($F_{10.7} \leq 120$, $F_{10.7}$_ave = 85) and high ($F_{10.7} > 120$, $F_{10.7}$_ave = 160) solar fluxes. We have three seasonal bins with 4 month period each: equinox (March, April, September, and October), December solstice (January, February, November, and December), and June solstice (May, June, July, and August).

3. Analysis and Results

3.1. Plasmaspheric Climatology

For our global analysis of the plasmaspheric TEC morphology, all the data from different seasons and longitudes were combined and averaged to produce plasmaspheric TEC maps in the magnetic latitude and local time coordinate for different geomagnetic and solar activities as shown in Figure 2. Figure 2 (top row)shows seasonally and longitudinally averaged pTEC maps for low (Figure 2, left column), medium (Figure 2, middle column), and high (Figure 2, right column) geomagnetic activity levels for low (Figure 2, top row) and high (Figure 2, bottom row) solar flux conditions. The range of the color scale for the pTEC maps is from 0 to

Table 1. Binning Criteria for Geomagnetic Activity, Solar Flux, Season, and the Geomagnetic Coordinate System

3 h *Kp* Index	$F_{10.7\ cm}$ Flux	Season (Month)	Magnetic Latitude and MLT
$Kp \leq 1.7$	$F_{10.7} < 120$	Equinox (3, 4, 9, and 10)	2 × 15 min
$2.0 \leq Kp \geq 3.0$	$F_{10.7} \geq 120$	June solstice (5, 6, 7, and 8)	
$Kp \geq 3.3$		December solstice (1, 2, 11, and 12)	

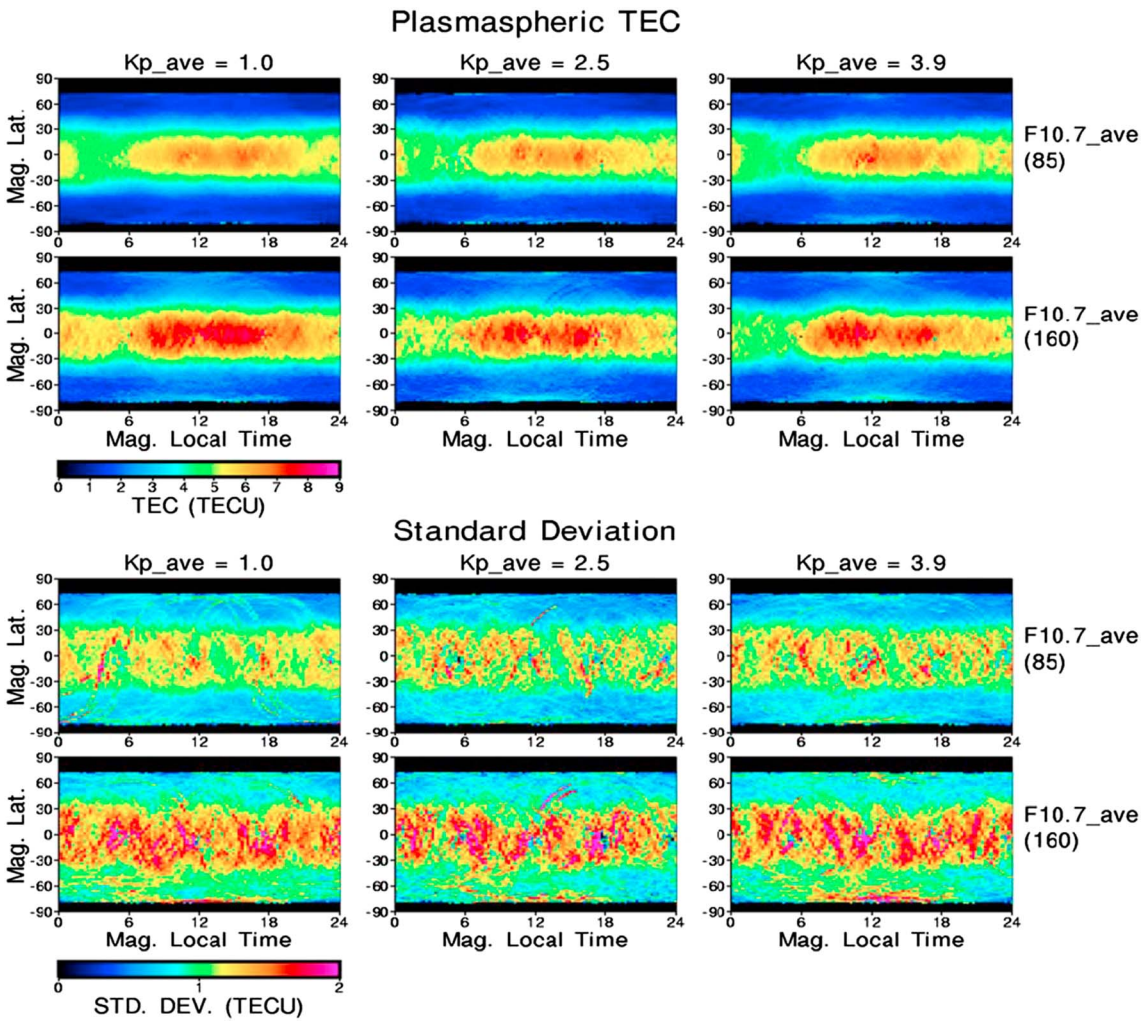

Figure 2. Seasonally and longitudinally averaged plasmaspheric TEC and standard deviation maps for (left column) low, (middle column) medium, and (right column) high geomagnetic activity levels for (top row) low and (bottom row) high solar activity conditions.

9 TECU (1 TECU = 10^{16} el/m^2). Figure 2 (bottom row) shows the standard deviations indicating the variabilities within each bin described. The color scale for the standard deviations ranges from 0 to 2 TECU.

The pTEC is noticeably larger for high solar flux conditions than for low solar flux conditions. As for the geomagnetic activity levels, the pTEC seems to be almost independent of the geomagnetic activity for low solar flux condition ($F_{10.7} < 120$, $F_{10.7ave} \sim 85$). For high solar flux condition ($F_{10.7} > 120$, $F_{10.7ave} \sim 160$), however, the pTEC decreases with increasing geomagnetic activity at low latitudes in the early morning sector of 00:00–06:00 MLT. At higher latitudes, on the other hand, pTEC slightly increases in the southern hemisphere. Note that the standard deviations are also simultaneously increasing as pTEC increases.

The pTEC shows clear latitude and local time variations. The largest pTEC occurs in the low latitudes and then it decreases as latitude increases, which is consistent with the spatial geometry of the plasmasphere. There are also noticeable local time variations, in particular at low latitudes: minimum pTEC occurs right before the sunrise and the daytime pTEC is mostly larger than the nighttime pTEC. For example, the averaged pTECs at low latitudes (−12° to 12°) are approximately 7 TECU and 5 TECU during the day (1400–1600 MLT) and night (0200–0400 MLT), respectively. At midlatitudes (45°–50° in magnetic latitude), however, the differences between the daytime and nighttime pTEC are relatively small.

Note that the local time variations of pTEC is significantly smaller than the local time variations of the ionospheric TEC although they both have similar variations with local time: minimum before sunrise,

enhancement toward the daytime maximum in the afternoon, and a slow decay in the evening [*Codrescu et al*., 1999; *Jee et al*., 2004; *Lee et al*., 2013]. For example, in the ionosphere, according to the results of *Jee et al*. [2004], TEC in the morning sector increases by about more than 100% from 10 to 20 TECU (20 to 40 TECU) for low (high) solar flux condition, while pTEC in the morning sector increases by only about 20% from 5 to 6 TECU (6 to 7 TECU) for low (high) solar flux condition. Also, the nighttime decay of pTEC is found to be much slower and less than the ionospheric TEC, particularly in the equatorial region. These differences were mostly confirmed at *Lee et al*. [2013] in the direct comparisons between the ionospheric and plasmaspheric TECs simultaneously measured from Jason 1 satellite.

The standard deviations of pTEC show little local time dependence except for the cases at higher latitudes for high solar flux, for which the daytime standard deviations are larger than the one at night. The large deviations occur in the low-latitude regions (−30°–30°) where pTEC itself is also large.

3.2. Seasonal and Solar Activity Variations

In order to study the seasonal variations of the plasmasphere, longitudinally averaged pTECs for equinox, December solstice, and June solstice are calculated and displayed in Figure 3. For each season, pTECs are shown for low (Figure 3, left column), medium (Figure 3, middle column), and high (Figure 3, right coloum) geomagnetic activity levels for low (Figure 3, top row) and high (Figure 3, bottom row) solar flux conditions. Each season consists of four months: equinox (March, April, September, and October), December solstice (January, February, November, and December), and June solstice (May, June, July, and August).

The local time variations of pTEC show little differences for all three seasons: that is, there is a minimum before sunrise, a relatively large increase toward a peak in the afternoon, and a slow decay at night [*Codrescu et al*., 1999; *Jee et al*., 2004]. In the low latitudes, the lowest pTECs occur for June solstice but the highest pTECs occur for equinox, in particular, for high solar flux condition, which are reminiscent of annual and semiannual anomalies in the ionosphere. At higher latitudes, greater than 45°. in latitude, pTECs for solstices are larger in the summer hemispheres than in the winter hemisphere for high solar flux condition. However, this hemispheric difference is hardly visible for low solar flux condition in Figure 3.

In order to see latitudinal and local time pTEC variations in more detail, Figures 4a–4c show the longitudinally averaged pTEC values plotted as a function of magnetic latitude at four local time sectors (02–04, 08–10, 14–16, and 20–22 MLT) from the TEC maps in Figure 3 for equinox, December solstice, and June solstice, respectively. The pTEC variations are simultaneously displayed for low (thin line) and high (thick line) solar flux conditions as indicated in the figure.

For equinox in Figure 4a, pTECs are almost symmetric around the peak at the geomagnetic equator, decreasing with increasing latitudes, except for the high-latitude boundary regions. Even for solstice periods, the low-latitude and midlatitude TECs are fairly symmetric in Figures 4b and 4c. However, the summer (southern) hemisphere in December shows larger TEC than in winter (northern) hemisphere, especially in the morning sector (0800–1000 MLT) for high solar flux condition. Note that the plasmaspheric density distribution is purely dependent on the coupling processes to the ionosphere during geomagnetically undisturbed periods and the coupling processes can be different in the summer and winter hemispheres. The larger TEC in summer hemisphere may indicate that there are more ionospheric plasma moving up to the plasmasphere in the summer hemisphere than in the winter hemisphere. The prevailing summer-to-winter interhemispheric wind for solstices may enhance the upward plasma flow from the ionosphere to the plasmasphere in the summer hemisphere, but it works reversely to reduce the plasmaspheric density in the winter hemisphere [*Evans and Holt*, 1978].

The density differences among the three seasons are almost negligible during low solar flux condition but, as is pointed out earlier with Figure 3, seasonal variations become noticeable for high solar flux condition. It is also noted that the density differences from low ($F_{10.7} \sim 85$) to high ($F_{10.7} \sim 160$) solar flux conditions are negligibly small comparing the ionosphere that shows more than a factor of 2 differences with similar solar flux change. The maximum difference is only about 2 TECU for equinox during low geomagnetic activity in Figure 4a, which is only about 30% increase from low to high solar flux. The differences are much smaller in other cases. This pTEC variation with solar flux condition indicates that the large

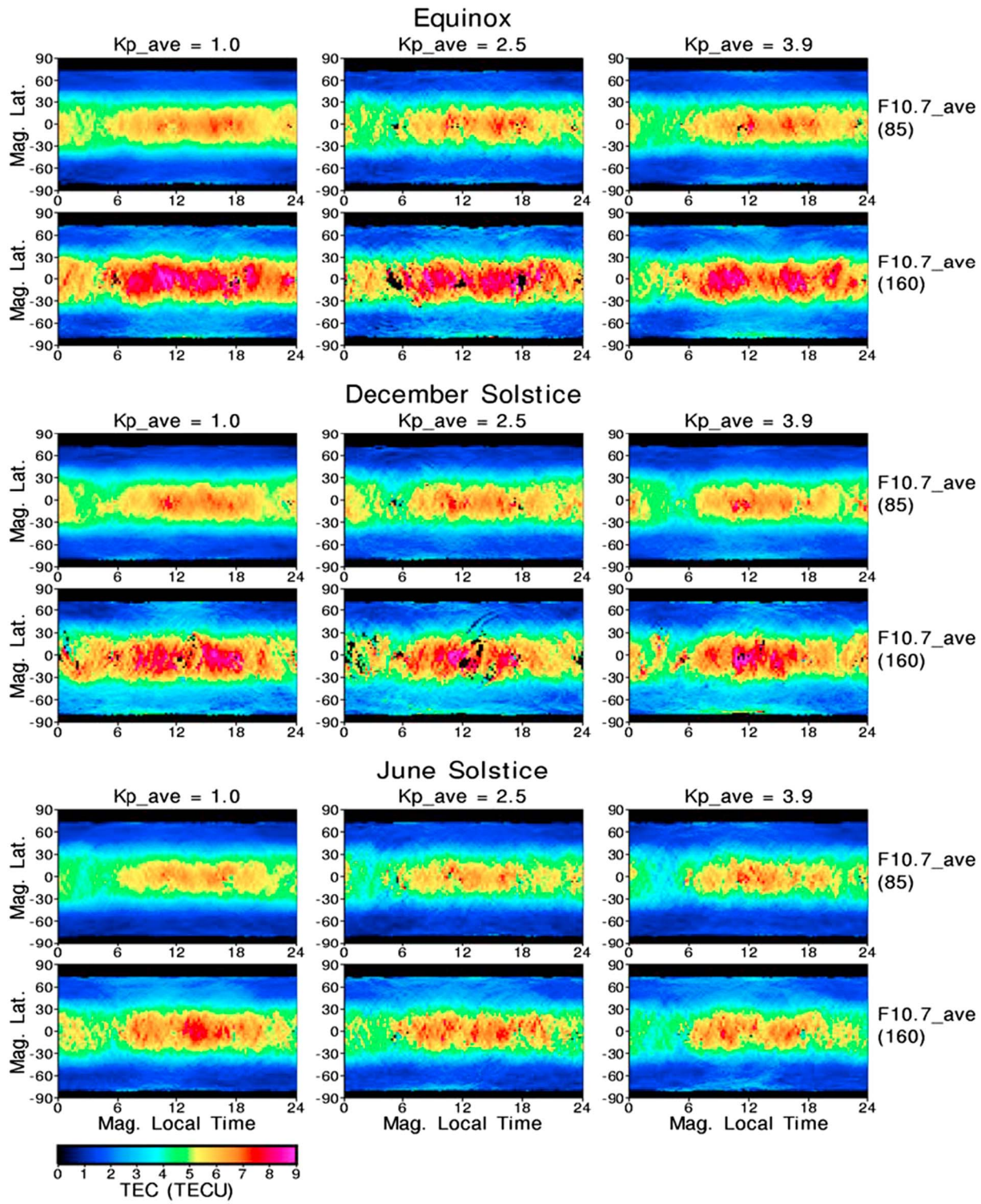

Figure 3. Longitudinally averaged pTEC maps for equinox, December solstice, and June solstice. For each season, pTECs are shown for (left column) low, (middle column) medium, and (right column) high geomagnetic activity levels for (top row) low and (bottom row) high solar activity conditions.

ionospheric density changes with solar flux are not reflected in the plasmasphere via a direct plasma transport between them. In other words, the daytime upward plasma transport from the ionosphere to the plasmasphere seems not to be necessarily enhanced with increasing solar flux even though the ionospheric density greatly increases.

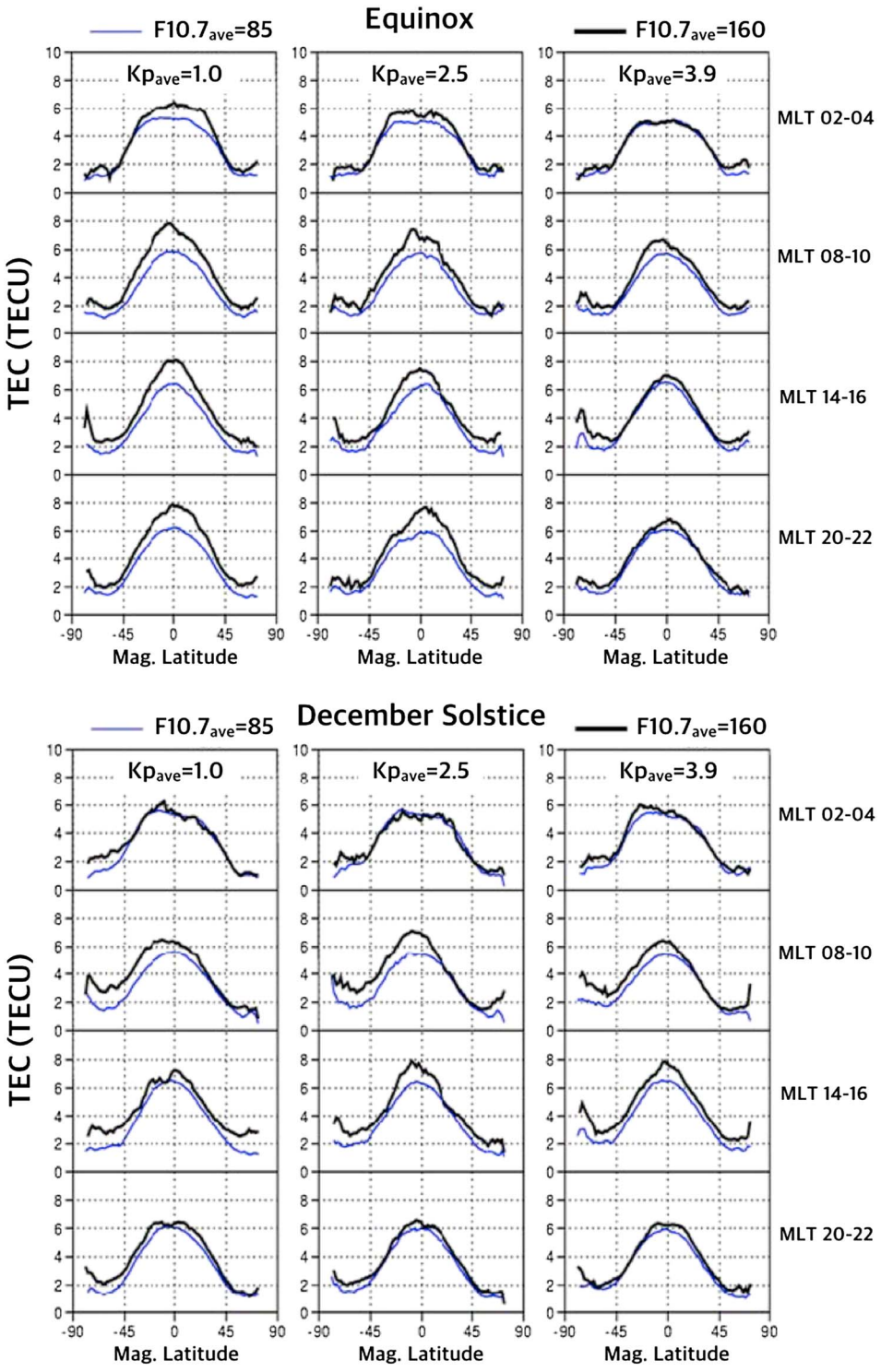

Figure 4. (a) Longitudinally averaged pTEC as a function of magnetic latitude during equinox at four given local time sectors (top to bottom). pTECs are shown for (left) low, (middle) medium, and (right) high geomagnetic activity levels. The thin and thick lines are for low and high solar activity conditions, respectively. (b) Same as Figure 4a but for December solstice. (c) Same as Figure 4a but for June solstice.

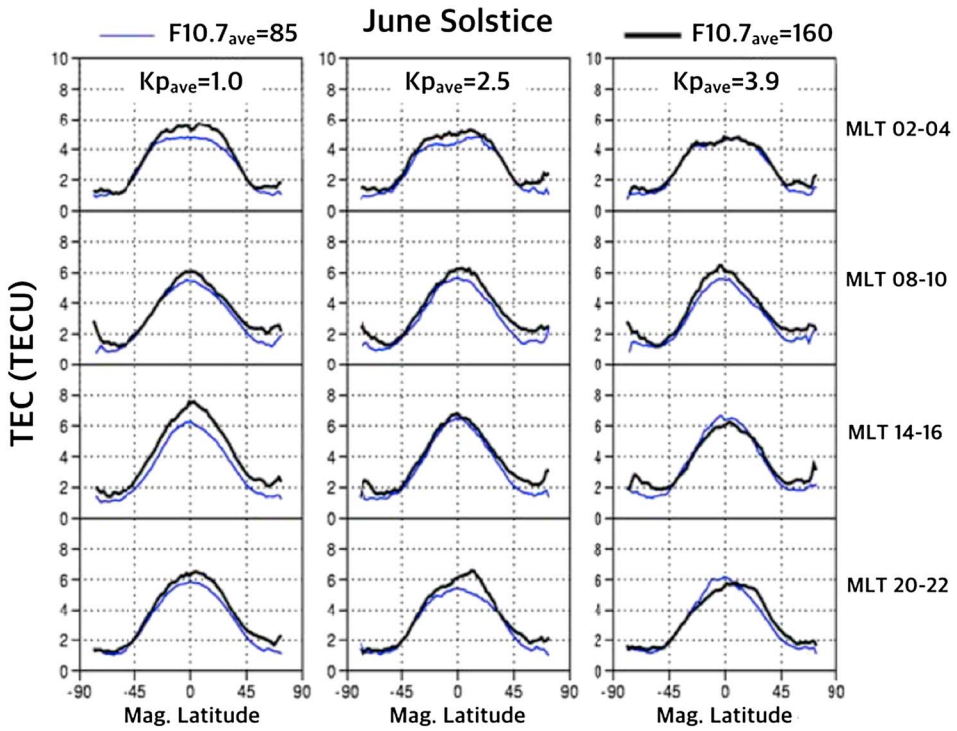

Figure 4. (continued)

3.3. Longitudinal Variations

So far, all of our results were pertained to longitudinally averaged conditions and no distinctions from longitude were made. Figure 5 shows seasonal TEC maps in three longitude sectors (in three columns) for geomagnetically quiet conditions ($Kp < 3.0$, Kp_ave = 1.67). The three selected longitude sectors include Pacific (150°–280°E), Atlantic (280°–30°E), and Indian (30°–150°E), and the choice of three longitude bins was motivated by the work of *Jee et al*. [2004]. For each season, Figure 5 (top and bottom) are for low and high solar flux conditions, respectively. The spots with black color in the low-latitude regions are the locations where no data points exist. For both low and high solar flux conditions, all three seasons show the apparent evidence of longitudinal dependence of pTEC. For example, the low-latitude pTECs in December are largest in the Atlantic sector, but in June, they are lowest in the same longitude sector.

In order to further investigate the latitudinal and local time dependences of the longitudinal pTEC variations, the pTEC maps are presented in the magnetic latitude and geographic longitude coordinate for geomagnetically quiet condition ($Kp < 3.0$, Kp_ave = 1.67) in Figure 6. TEC maps for daytime (0060–1800 MLT) and nighttime (0000–0600 MLT) are separately presented for each season and solar flux condition as indicated in the figure. The relatively large local time bins were applied to have a good data coverage. Note that reducing the bin sizes (for example, 1200–1500 MLT and 0000–0300 MLT) does not make any noticeable difference.

As is found in Figure 5, TEC maps in Figure 6 exhibit significant longitudinal variations in the low-latitude region with noticeable seasonal discrepancies. The most notable features are wide equatorial density peak and trough occurring at around 300°E longitude in December and June solstices, respectively. This feature is particularly noticeable at night. Figures 7a–7c show scatterplots of the nighttime and daytime pTECs versus geographic longitude for equinox (Figure 7a), December solstice (Figure 7b), and June solstice (Figure 7c). The three columns of the scatterplots correspond to the southern middle latitudes (−50 to −45), low latitudes (−12–12), and northern middle latitudes (45–50) from left to right. Superimposed in each plot are the average TECs and standard deviations around them as error bars. These scatterplots clearly exhibit December peaks and June troughs at around 300°E longitude both during the day and night in Figures 7b and 7c, respectively, which can be interpreted as an annual anomaly in the plasmasphere. The annual

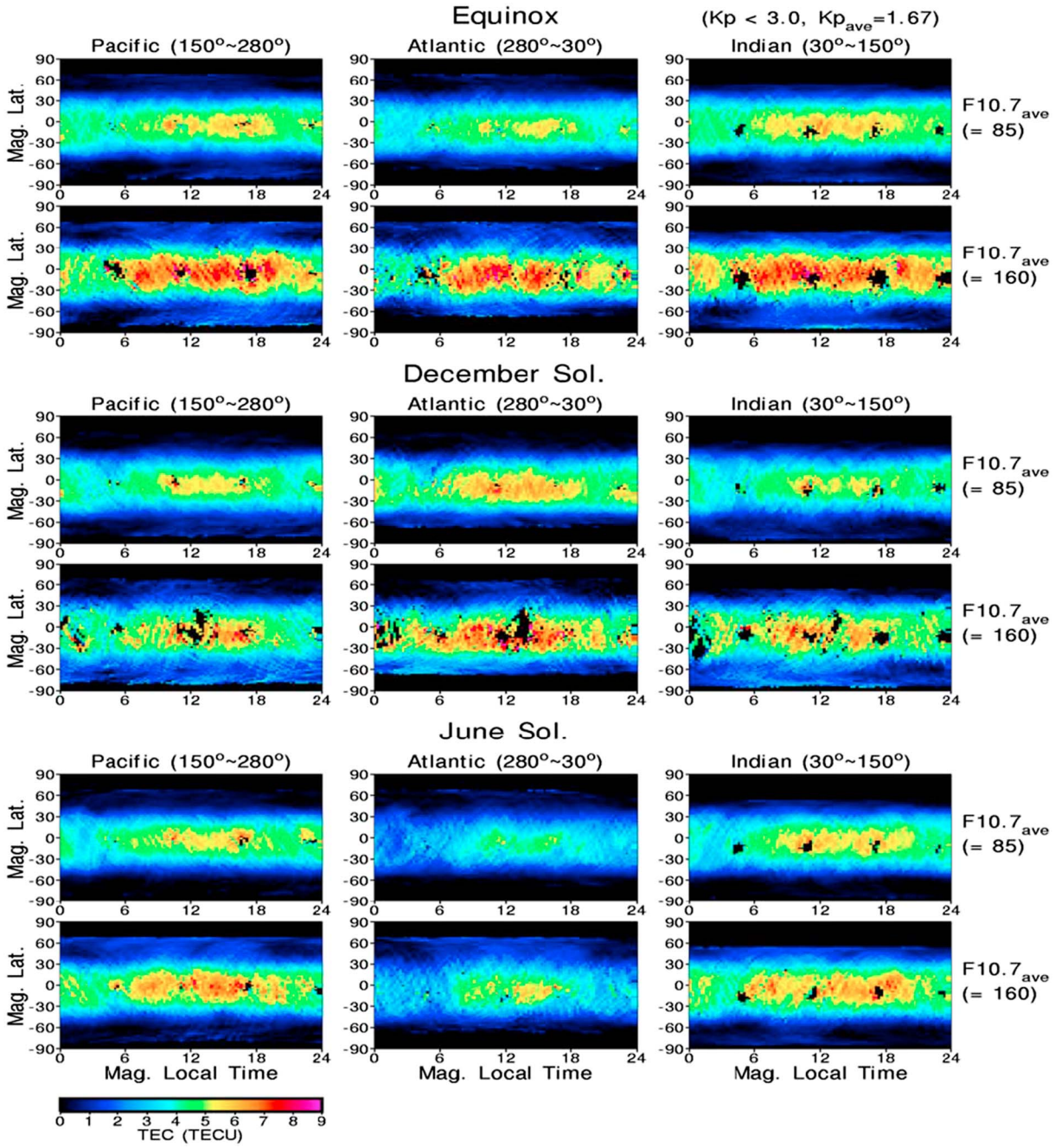

Figure 5. Seasonal pTEC maps in three longitude sectors (in three columns) for geomagnetically quiet condition ($Kp < 3.0$, $Kp\_ave = 1.67$). For each season, top and bottom plots are for low and high solar activity conditions, respectively.

anomaly in the plasmasphere has been reported in previous studies [*Park*, 1974; *Park et al*., 1978; *Clilverd et al*., 1991; *Guiter et al*., 1995; *Richards et al*., 2000; *Clilverd et al*., 2007; *Menk et al*., 2012; *Lee et al*., 2013]. However, the global picture of the annual anomaly in the plasmasphere was not available until Jason 1 satellite observation provides the plasmaspheric pTEC over the entire period of declining phase of solar cycle. *Clilverd et al*. [2007] found that the largest annual variation occurred at American longitudes, but only using CRRES satellite measurements of equatorial electron density in the range of L = 2.5–5.0 during the solar maximum period of 1990–1991. *Menk et al*. [2012] also found similar result using satellite in situ measurements of electron densities for solar maximum period. The present study showed that the annual

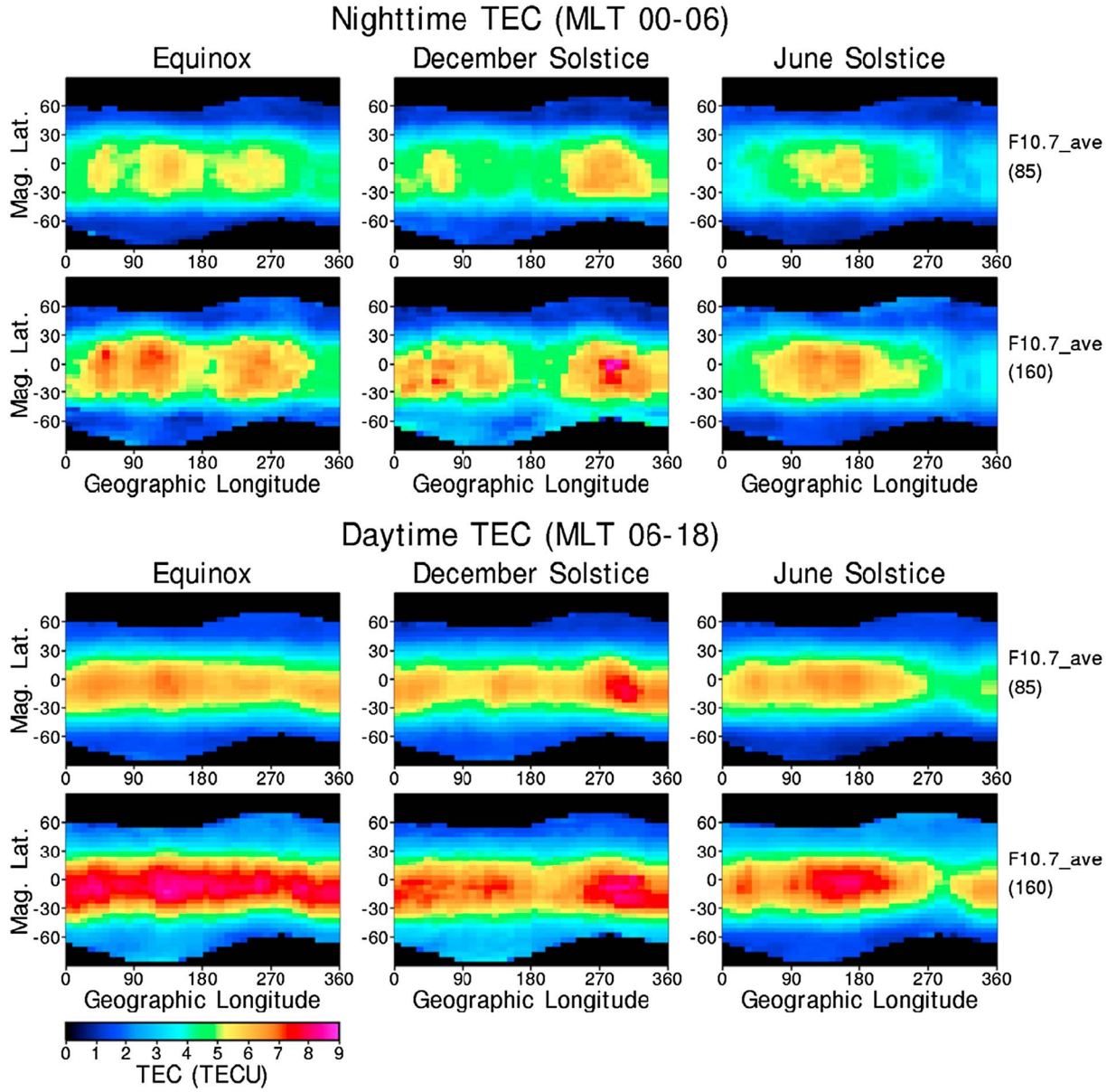

Figure 6. Nighttime and daytime pTEC maps as a function of magnetic latitude and geographic longitude for three seasons (in columns) during geomagnetically quiet condition ($Kp < 3.0$, $Kp\_ave = 1.67$). For each time period, top and bottom plots are for low and high solar activity conditions, respectively.

variation over the American sector results from the longitudinal variations with almost opposite phase for December and June solstices, regardless of solar activity.

For equinox (Figure 7a), there are also significant longitudinal variations particularly in the nighttime equatorial region but almost negligible during the day. In the midlatitude plasmasphere, the longitudinal variations are negligibly small except for the nighttime high solar flux conditions which show discernable variations in the northern midlatitude ($45° <$ magnetic latitude (MLAT) $< 50°$) for equinox (Figure 7a) and in the southern midlatitude ($-50° <$ MLAT $< -45°$) for December solstice (Figure 7b).

There are two major factors influencing the longitudinal variations of the ionosphere: magnetic declination and forcing from the lower atmosphere. The magnetic declination works with the neutral winds to affect the longitudinal variations of the electron density in the midlatitude ionosphere. The relatively large longitudinal variation of the magnetic declination, in particular, in the southern hemisphere is closely related to the longitudinal variation of plasma transport by the zonal component of the neutral wind, which results in the

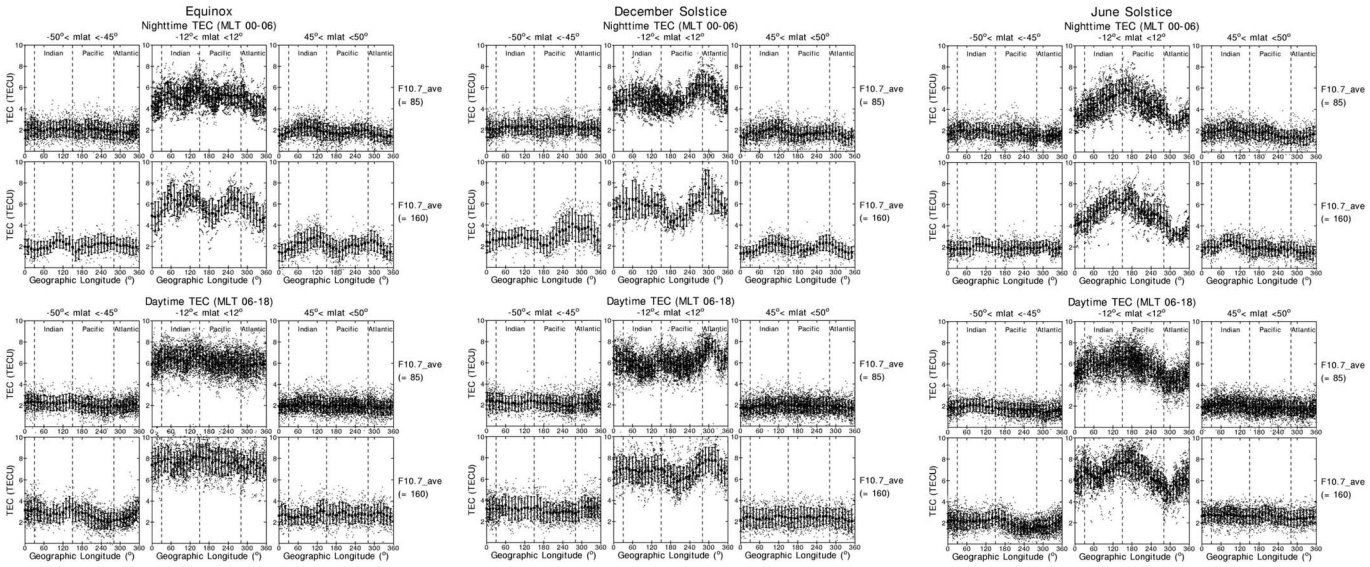

Figure 7. (a) Scatterplots for nighttime and daytime pTEC as a function of geographic longitude for three magnetic latitude regions (in columns) for equinox during geomagnetically quiet condition ($Kp < 3.0$, $Kp\_ave = 1.67$). For each time period, top and bottom plots are for low and high solar activity conditions, respectively. The black squares represent average values, and the vertical bars show standard deviations. (b) Same as Figure 7a but for December solstice. (c) Same as Figure 7a but for June solstice.

longitudinal variations of the midlatitude ionospheric density such the Weddell Sea Anomaly [*Horvath*, 2006; *Jee et al*., 2009]. The lower atmospheric forcing propagates upward into the upper atmosphere in form of the atmospheric waves, such as gravity wave and tide, to produce significant variations of the ionospheric density with longitude in the equatorial region [e.g., *Sagawa et al*., 2005; *Immel et al*., 2006; *Kil et al*., 2007; *Kim et al*., 2008]. However, we have not found any such corresponding longitudinal variations in the plasmasphere. This result indicates that the plasmaspheric density is not linearly correlated with the ionospheric density although the coupling to the ionosphere is the main factor to control the plasmaspheric density distributions.

3.4. Geomagnetic Activity Variations

Figures 2–4 present the pTEC variations with geomagnetic activity. For $F_{10.7} < 120$, there are slight TEC enhancements at high latitudes in the southern hemisphere and also small decrease at low latitudes in the early morning sector, but the overall morphology of pTEC seems to be largely independent of geomagnetic activity. For $F_{10.7} > 120$, pTECs are found to decrease with geomagnetic activity at low latitudes, especially for equinox (see Figure 4a), but it slightly increases at high latitudes in the southern hemisphere (see Figure 3). In the midlatitude region, however, pTEC variations are nearly negligible (see Figure 4). On the whole, pTEC variations with geomagnetic activity are relatively small. The plasmasphere is known to experience a density depletion via the erosion of plasma during geomagnetic storm. However, the erosion process occurs in the outermost part of the plasmasphere in which the plasma density is small, and therefore, its contribution to pTEC may not be large enough to be noticed in the pTEC climatology.

4. Summary and Conclusion

The total electron content of the plasmasphere (1336–20,200 km altitude region) had been measured by the GPS receiver on board the Jason 1 satellite during the declining phase of solar cycle 23 from 2002 to 2008. The statistical analysis of the data provides the overall characteristics of the plasmaspheric density, specifically the density variations with latitude and longitude, local time, season, and solar and magnetic activities:

1. Local time: a minimum density occurs just before sunrise. The density increases after sunrise toward the broad peak in the afternoon and then a slow decay after sunset. The density difference between the day and night is not as large as in the ionosphere.

2. Season: the low-latitude plasmaspheric density is overall lowest for June solstice and highest for equinox, which is similar to the annual and semiannual anomalies in the ionosphere, but this seasonal variation is almost negligible for low solar flux condition. There are hemispheric asymmetries in the plasmaspheric density for solstices: in general, the summer hemisphere shows larger density than the winter hemisphere.
3. Solar activity: the plasmaspheric density increases by about 10–30% with solar activity, but the change is relatively small compared with the large ionospheric density change of more than 100%.
4. Latitude: the maximum density occurs over the magnetic equator and then decreases with latitude.
5. Longitude: there are significant variations with longitude in the plasmasphere. In particular, the variations for solstices show very systematic differences, which results in strong annual asymmetry (being greater in December than in June) in the American sector (around 300°E).
6. Geomagnetic activity: the plasmaspheric density shows little variation with geomagnetic activity for low solar flux condition. For high solar flux condition, however, the equatorial density decreases with geomagnetic activity but it slightly increases in the southern high-latitude region. The midlatitude pTEC variations are nearly negligible regardless of solar flux condition.

Considering the close coupling between the plasmasphere and the ionosphere, it is expected that the state of the ionosphere should be somewhat reflected in the plasmasphere. However, the results of this study showed that the characteristics of plasmaspheric TEC is significantly different from the ionosphere. This indicates that the coupling processes between the two regions are not simple and linear to directly connect one to the other region. Moreover, it is further complicated by the storm time depletion of the plasmaspheric density into the outer space. For better understanding of the coupling processes between the ionosphere and the plasmasphere, it would be necessary to have more observations not only for the plasmaspheric TEC but also for plasma density profiles with height if available.

Acknowledgments
This study was supported by the grant PE17020 from Korea Polar Research Institute. The Jason 1 TEC data are obtained from the Physical Oceanography Distributed Active Archive Center at the NASA Jet Propulsion Laboratory (http://podaac.jpl.nasa.gov).

References

Belehaki, A., N. Jakowski, and B. W. Reinisch (2004), Plasmaspheric electron content derived from GPS TEC and digisonde ionograms, *Adv. Space Res.*, *33*, 833–837, doi:10.1016/j.asr.2003.07.008.

Bishop, G. J., J. A. Secan, and S. H. Delay (2009), GPS TEC and the plasmasphere: Some observations and uncertainties, *Radio Sci.*, *44*, RS0A26, doi:10.1029/2008RS004037.

Carpenter, D. L., and C. G. Park (1973), On what ionospheric workers should know about the plasmaspause-plasmasphere, *Rev. Geophys. Space Phys.*, *11*, 133–154, doi:10.1029/RG011i001p00133.

Clilverd, M. A., A. J. Smith, and N. R. Thomson (1991), The annual variation in quiet time plasmaspheric electron density, determined from whistler mode group delays, *Planet. Space Sci.*, *39*, 1059–1067, doi:10.1016/0032-0633(91)90113-O.

Clilverd, M. A., N. P. Meredith, R. B. Horne, S. A. Glauert, R. R. Anderson, N. R. Thomson, F. W. Menk, and B. R. Sandel (2007), Longitudinal and seasonal variations in plasmaspheric electron density: Implications for electron precipitation, *J. Geophys. Res.*, *112*, A11210, doi:10.1029/2007JA012416.

Codrescu, M. V., S. E. Palo, X. Zhang, T. J. Fuller-Rowell, and C. Poppe (1999), TEC climatology derived from TOPEX/POSEIDON measurements, *J. Atmos. Sol. Terr. Phys.*, *61*, 281–298, doi:10.1016/S1364-6826(98)00132-1.

Codrescu, M. V., K. L. Beierle, T. J. Fuller-Rowell, S. E. Palo, and X. Zhang (2001), More total electron content climatology from TOPEX/Poseidon measurements, *Radio Sci.*, *36*, 325–333, doi:10.1029/1999RS002407.

Evans, J. V., and J. M. Holt (1978), Nighttime proton fluxes at Millstone Hill, *Planet. Space Sci.*, *26*, doi:10.1016/0032-0633(78)90004-1.

Fu, L. L., E. J. Christensen, and C. A. Yamarone Jr. (1994), TOPEX/Poseidon mission overview, *J. Geophys. Res.*, *99*, 24,369–24,381, doi:10.1029/94JC01761.

Ganguli, G., M. A. Reynolds, and M. W. Liemohn (2000), The plasmasphere and advances in plasmaspheric research, *J. Atmos. Sol. Terr. Phys.*, *61*, 1647–1657, doi:10.1016/S1364-6826(00)00117-6.

Guiter, S. M., C. E. Rasmussen, T. I. Gombosi, J. J. Sojka, and R. W. Schunk (1995), What is the source of observed annual variations in plasmaspheric density?, *J. Geophys. Res.*, *91*, 8013–8020, doi:10.1029/94JA02866.

Horvath, I. (2006), A total electron content space weather study of the nighttime Weddell Sea Anomaly of 1996/1997 southern summer with TOPEX/Poseidon radar altimetry, *J. Geophys. Res.*, *111*, A12317, doi:10.1029/2006JA011679.

Horwitz, J. L., L. H. Brace, R. H. Comport, and C. R. Chappell (1986), Dual-spacecraft measurements of plasmasphere-ionosphere coupling, *J. Geophys. Res.*, *91*, 11,203–11,216, doi:10.1029/JA091iA10p11203.

Huba, J., and J. Krall (2013), Modeling the plasmasphere with SAMI3, *Geophys. Res. Lett.*, *40*, 6–10, doi:10.1029/2012GL054300.

Immel, T. J., E. Sagawa, S. L. England, S. B. Henderson, M. E. Hagan, S. B. Mende, H. U. Frey, C. M. Swenson, and L. J. Paxton (2006), Control of equatorial ionospheric morphology by atmospheric tides, *Geophys. Res. Lett.*, *33*, L15108, doi:10.1029/2006GL026161.

Jee, G., R. W. Schunk, and L. Scherliess (2004), Analysis of TEC data from the TOPEX/Poseidon mission, *J. Geophys. Res.*, *109*, A01301, doi:10.1029/2003JA010058.

Jee, G., A. G. Burns, Y.-H. Kim, and W. Wang (2009), Seasonal and solar activity variations of the Weddell Sea Anomaly observed in the TOPEX total electron content measurements, *J. Geophys. Res.*, *114*, A04307, doi:10.1029/2008JA013801.

Jee, G., H.-B. Lee, Y. H. Kim, J.-K. Chung, and J. Cho (2010), Assessment of GPS global ionosphere maps (GIM) by comparison between CODE GIM and TOPEX/Jason TEC data: Ionospheric perspective, *J. Geophys. Res.*, *115*, A10319, doi:10.1029/2010JA015432.

Kil, H., S.-J. Oh, M. C. Kelley, L. J. Paxton, S. L. England, E. Talaat, K.-W. Min, and S.-Y. Su (2007), Longitudinal structure of the vertical E × B drift and ion density seen from ROCSAT-1, *Geophys. Res. Lett.*, *34*, L14110, doi:10.1029/2007GL030018.

Kim, E., G. Jee, and Y. H. Kim (2008), Seasonal characteristics of the longitudinal wavenumber-4 structure in the equatorial ionospheric anomaly, *J. Astron. Space Sci.*, *25*(4), 335–346, doi:10.5140/JASS.2008.25.4.335.

Kutiev, I., and P. Marinov (2007), Topside sounder model of scale height and transition height characteristics of the ionosphere, *Adv. Space Res.*, *39*, 759–766, doi:10.1016/j.asr.2006.06.013.

Kutiev, I., S. Stankov, and P. Marinov (1994), Analytical expression of O^+-H^+ ion transition surface for use in IRI, *Adv. Space Res.*, *14*, (12)135–(12)138.

Lee, H.-B., G. Jee, Y. H. Kim, and J. S. Shim (2013), Characteristics of global plasmaspheric TEC in comparison with the ionosphere simultaneously observed by Jason-1 satellite, *J. Geophys. Res. Space Physics*, *118*, 935–946, doi:10.1002/jgra.50130.

Mannucci, A. J., B. D. Wilson, and C. D. Edwards (1993), A new method for monitoring the Earth's ionospheric total electron content using the GPS global network. *Proceedings of ION GPS-93, the 6th International Technical Meeting of the Satellite Division of The Institute of Navigation, Salt Lake City, UT, 22–24 September*, The Institute of Navigation, Alexandria, VA, pp. 1323–1332.

Marinov, P., I. Kutiev, and S. Watanabe (2004), Empirical model of O^+-H^+ transition height based ontopside sounder data, *Adv. Space Res.*, *34*, 2021–2025, doi:10.1016/j.asr.2004.07.012.

Mazzella, A. J., Jr. (2009), Plasmasphere effects for GPS TEC measurements in North America, *Radio Sci.*, *44*, RS5014, doi:10.1029/2009RS004186.

Menk, F. W., S. T. Ables, R. S. Grew, M. A. Clilverd, and B. R. Sandel (2012), The annual and longitudinal variations in plasmaspheric ion density, *J. Geophys. Res.*, *117*, A03215, doi:10.1029/2011JA017071.

Park, C. G. (1973), Whistler observations of the depletion of the plasmasphere during a magnetospheric substorm, *J. Geophys. Res.*, *78*, 672–683, doi:10.1029/JA078i004p00672.

Park, C. G. (1974), Some features of plasma distribution in the plasmasphere deduced from Antarctic whistlers, *J. Geophys. Res.*, *79*(1), 169–173, doi:10.1029/JA079i001p00169.

Park, C. G., D. L. Carpenter, and D. B. Wiggin (1978), Electron density in the plasmasphere: Whistler data on solar cycle, annual, and diurnal variations, *J. Geophys. Res.*, *83*, 3137–3144, doi:10.1029/JA083iA07p03137.

Richards, P. G., T. Chang, and R. H. Comfort (2000), On the causes of the annual variation in the plasmaspheric electron density, *J. Atmos. Sol. Terr. Phys.*, *62*, 935–946, doi:10.1016/S1364-6826(00)00039-0.

Sagawa, E., T. J. Immel, H. U. Frey, and S. B. Mende (2005), Longitudinal structure of the equatorial anomaly in the nighttime ionosphere observed by IMAGE/FUV, *J. Geophys. Res.*, *110*, A11302, doi:10.1029/2004JA010848.

Sandel, B. R., and M. H. Denton (2007), Global view of refilling of the plasmasphere, *Geophys. Res. Lett.*, *34*, L17102, doi:10.1029/2007GL030669.

Scherliess, L., D. C. Thompson, and R. W. Schunk (2008), Longitudinal variability of low-latitude total electron content: tidal influences, *J. Geophys. Res.*, *113*, A01311, doi:10.1029/2007JA012480.

Singh, U. P., and R. P. Singh (1997), Study of plasmasphere-ionosphere coupling fluxes, *J. Atmos. Sol. Terr. Phys.*, *59*, 1321–1327, doi:10.1016/S1364-6826(96)00171-X.

Thompson, D. C., L. Scherliess, J. J. Sojka, and R. W. Schunk (2009), Plasmasphere and upper ionosphere contributions and corrections during the assimilation of GPS slant TEC, *Radio Sci.*, *44*, RS0A02, doi:10.1029/2008RS004016.

Vladimer, J. A., P. Jastrzebski, M. C. Lee, P. H. Doherty, D. T. Decker, and D. N. Anderson (1999), Longitude structure of ionosphere total electron content at low latitudes measured by the TOPEX/Poseidon satellite, *Radio Sci.*, *34*, 1239–1260, doi:10.1029/1999RS900060.

Webb, P. A., and E. A. Essex (2004), A dynamic global model of the plasmasphere, *J. Atmos. Sol. Terr. Phys.*, *66*, 1057–1073, doi:10.1016/j.jastp.2004.04.001.

Yizengaw, E., M. B. Moldwin, D. Galvan, B. A. Iijima, A. Komigathy, and A. J. Mannucci (2008), Global plasmaspheric TEC and its relative contribution to GPS TEC, *J. Atmos. Sol. Terr. Phys.*, *70*, 1541–1548, doi:10.1016/j.jastp.2008.04.022.